

CloudSat/CPRおよびCALIPSO/CALIOP観測による雲・降水粒子タイプ 識別アルゴリズムの開発

Algorithm Development for Discriminating Cloud and Precipitation Particle Type using CloudSat/CPR and CALIPSO/CALIOP Observation

*菊池 麻紀¹、岡本 創²、佐藤 可織²、萩原 雄一郎¹

*Maki Kikuchi¹, Hajime Okamoto², Kaori Sato², Yuichiro Hagihara¹

1. 宇宙航空研究開発機構、2. 九州大学

1. Japan Aerospace Exploration Agency, 2. Kyushu University

Cloud and precipitation take key roles in the climate system. Information on the cloud phase, shape, rain and snow (hereafter, hydrometeor particle types) are among the major factors that determine the radiative properties of cloud and precipitation. The knowledge on the hydrometeor types is also necessary to retrieve their microphysical properties, such as liquid/ice/rain/snow water contents and effective radius. In this study, we developed an algorithm that discriminate the hydrometeor particle types using the cloud profiling radar (CPR) onboard CloudSat and Mie-scattering lidar, Cloud-Aerosol Lidar with Orthogonal Polarization (CALIOP), onboard Cloud-Aerosol Lidar and Infrared Pathfinder Satellite Observation (CALIPSO). The CloudSat and CALIPSO satellites are in operation since June 2006 and they have accumulated vertical profiles of cloud and precipitation over the globe for ten years. The CALIOP is sensible to thin to moderately thick clouds and the CPR is sensible to moderately thick clouds to light precipitation. Therefore, the development of the synergetic algorithm that discriminate hydrometeor particle types for the CPR and CALIOP observation would not only derive the global picture of cloud-precipitation typing but also would offer opportunities to further study the cloud-precipitation process and to evaluate its representativeness in global and regional numerical models.

The CALIOP cloud particle type discrimination algorithm was based on the previous scheme originally developed by Yoshida et al. [2010] and modified by Hiraoka et al. [2014]. The CPR algorithm consisted of three main steps: (1) initial type classification by radar reflectivity and European Center for Medium-range Weather Forecasting (ECMWF) temperature; (2) cloud-precipitation partitioning correction by attenuation corrected surface radar reflectivity; and (3) spatial continuity test. The initial type classification was conducted by selecting a type from a look-up-table of radar reflectivity and temperature. The look-up-table was constructed using the cloud particle type discrimination from CALIOP and the precipitation detection by Precipitation Radar (PR) onboard Tropical Rainfall Measuring Mission (TRMM). For each CloudSat bin, an initial type was selected from the look-up-table that corresponded to the observed radar reflectivity and ECMWF temperature. The second step was the cloud-precipitation partitioning correction where each profile was determined whether it was a precipitating profile or not by a simple threshold method of attenuation corrected surface radar reflectivity (Haynes et al. [2009]). If the profile was detected as precipitation but the initial classification had been registered as a cloud profile, the initial classification of the lowest hydrometeor classification was corrected to precipitation (and visa-versa). The last step of the CPR algorithm was the spatial continuity test to eliminate spike misclassification. The final CPR-CALIOP synergy scheme classified the hydrometeor particles into 13 types: warm water, supercooled water, randomly oriented ice crystals (3D-ice), horizontally oriented plates (2D-plate), 3D-ice + 2D-plate, liquid drizzle, solid drizzle, rain, snow, mixed phase, water+liquid drizzle, water+rain and unknown. Taking the advantage of CPR's capability to penetrate cloud and light precipitation and CALIOP's capability to detect thin clouds, the synergy algorithm derived the global

vertically resolved distribution of hydrometeor particle types from thin cirrus clouds to light precipitation.

The hydrometeor particle type algorithm is considered to be applied in upcoming Earth Clouds, Aerosols and Radiation Explorer (EarthCARE) Level 2 Standard Products that will be processed and released from JAXA to observe global and vertical distribution of the hydrometeor particle types.

キーワード：雲レーダ、ライダ、衛星、雲観測、降水観測

Keywords: cloud radar, lidar, satellite, cloud observation, precipitation observation

A long term calibration of space-borne precipitation radar using natural target

*金丸 佳矢¹、久保田 拓志²、井口 俊夫³、高薮 縁¹、沖 理子²

*Kaya Kanemaru¹, Takuji Kubota², Toshio Iguchi³, Yukari Takayabu¹, Riko Oki²

1. 東京大学大気海洋研究所、2. 宇宙航空研究開発機構 地球観測研究センター、3. 情報通信研究機構

1. Atmosphere and Ocean Research Institute, The University of Tokyo, 2. Earth Observation Research Center, Japan Aerospace Exploration Agency, 3. National Institute of Information and Communications Technology

Precipitation observation by the Tropical Rainfall Measuring Mission's (TRMM's) Precipitation Radar (PR) has lasted for almost 17 years. On February 28, 2014, the core satellite of the Global Precipitation Measurement (GPM) mission was launched, and the GPM Dual-frequency Precipitation Radar (DPR) started providing precipitation data succeeding the TRMM PR observation. PR and DPR not only estimate precipitation accurately both over land and the oceans but also provide information to derive precipitation characteristics (e.g., rain top height and rain vertical profile). Homogeneity of long-term PR/DPR data will be essential to study the water cycle change related to the decadal climate variability. Then, a long-term stability of calibration accuracy for radars is an important factor to correctly obtain the nature variability. The radar algorithm for precipitation estimates converts from the observed radar reflectivity factor, Z , to the estimated rain rate, R , so that a Z bias of calibration error is a cause of absolute error of R . On the other hand, a temporal change of calibration bias causes an artificial trend of R . Therefore, the long term trend of calibration error (calibration drift) must be evaluated and compensated. In this study, we develop a method of calibration drift estimates. While the normalized radar cross section (NRCS or sigma-zero) over water surface is related with sea surface wind (SSW), sigma-zero at small incident angles is insensitive at moderate (8-10 m/s) wind speeds. Since a relationship between sigma-zero and SSW is invariant, a temporal change of sigma-zero filtered by moderate winds is obtained as the calibration drift of radars. In this study, calibration drift of the PR version 7 (V7) product is evaluated using SSW data by the TRMM microwave imager (TMI). The calibration drift of the PR is found for a 0.2 dB change during the entire TRMM mission. The long-term trend of unconditional rain by the PR V7 over the TRMM coverage is overall caused by the calibration drift. The calibration drift of the PR found in the current study will be compensated in future (version 8; V8) product.

キーワード：降水レーダ、校正

Keywords: Precipitation radar, Calibration

Estimating vertical profile of water-cloud droplet effective radius from SWIR measurements of Himawari-8 via cloud profile statistics

*永尾 隆¹、中島 孝²

*Takashi M. Nagao¹, Takashi Y. Nakajima²

1. 宇宙航空研究開発機構地球観測研究センター、2. 東海大学情報技術センター

1. Earth Observation Research Center, Japan Aerospace Exploration Agency, 2. Tokai University Research and Information

Remote sensing of clouds by geostationary meteorological satellites with multispectral visible-to-infrared imaging capabilities by improved spectral, spatial and temporal resolution (e.g. Himawari-8/AHI, GOES-R/ABI) have potential to advance scientific understanding of cloud and precipitation process, by quantifying spatio-temporal distributions and evolutions of cloud radiative and microphysical properties such as cloud optical thickness (COT), cloud droplet effective radius (CDER), and cloud top temperature (CTT) and height (CTH). However, limitation of passive remote sensing to provide vertically-resolved cloud information including in-cloud CDER vertical profile (CDER-VP), drizzling existence, cloud geometric thickness and base height is one of the barriers to advancing our understanding of cloud and precipitation process.

This study developed an algorithm to retrieve CDER-VP of water cloud from shortwave infrared (SWIR) measurements of Himawari-8/AHI via cloud statistical profiles derived from CloudSat/CPR observation towards continuous monitoring of temporal evolution of clouds by Himawari-8. Several similar algorithms in previous studies utilize a spectral radiance matching on the assumption of simultaneous observation of radar and visible-to-infrared imagery such as CloudSat/CPR and Aqua/MODIS. However, note that, since our aim is to apply the algorithm to Himawari-8/AHI measurements, the algorithm does not assume simultaneous observations with CloudSat/CPR.

First, in advance, a database (DB) of CDER-VP is prepared by the following procedure: Top-of-atmosphere (TOA) radiances at three spectral bands (0.65, 2.3, 11- μm) of AHI are simulated from CDER-VP contained in CloudSat Radar-Visible Optical Depth Cloud Water Content Product (2B-CWC-RVOD) and cloud optical depth vertical profile in contained in CloudSat 2B-TAU product. COT, CDER and CTT are retrieved from the simulated radiances using an algorithm in assuming plane-parallel cloud structure (Nakajima and Nakajima, 1995). A set of the COT, CDER and CTT retrievals and inputted CDER-VP is added to the DB. Finally the algorithm retrieves CDER-VP from actual AHI measurement by the following procedure: COT, CDER and CTT are retrieved from the AHI radiances at 0.64, 2.3, 10.4- μm bands. Using the COT, CDER and CTT retrievals as key of the DB, multiple CDER-VPs are extracted from the DB. Using principal component (PC) analysis, up to three PC vectors of the CDER-VPs are extracted. Again, CDER-VP, COT, and CTT are retrieved from the AHI 0.64, 1.6, 2.3, 3.9 and 10.4- μm using the PC vectors of CDER-VPs with iterative radiative transfer calculation. Note that the sum of the contribution ratios of the three principal components vectors exceeds 95%.

This study evaluated the algorithm based on the simulation using the CloudSat 2B-CWC-RVOD and 2B-TAU products. The column mean CDERs calculated from the retrieved CDER-VPs are almost unbiased while the CDERs retrieved with the plane-parallel assumption have significant underestimation called so-called plane-parallel bias. The CDER-VP retrieval errors are almost smaller than 3- μm . The retrieval errors of the cloud base CDERs are almost larger than the others. The tendency can be explained by less sensitivity of SWIRs to CDER at cloud base.

Additionally, as a case study, this study will attempt to apply the algorithm to the AHI's high-frequency observations, and to interpret the time series of the CDER-VP retrievals in terms of temporal evolution of

water clouds.

Understanding sea surface temperature forcing of precipitation variability in the tropics

*Jie He¹

1. Princeton University

The great dependence of human society and natural ecosystems on rainfall makes precipitation variability an essential aspect of the earth's climate. In the tropics, it is well accepted that the ocean plays a crucial role in precipitation variability through variations in sea surface temperatures (SSTs). Above normal SSTs often increase the boundary-layer moist static energy and induce anomalous convection. An important yet unresolved question is: how strong is the SST forcing? Observational studies have long suggested an intense SST forcing for base SSTs around 27.5°C but little forcing for very high base SSTs. In this seminar, I will show that simultaneous SST-rainfall relationships in any coupled system, including observations, are inadequate for quantifying the SST forcing. This is largely due to the two-way interplay between the atmosphere and ocean. Results from uncoupled simulations show that the SST forcing in fact becomes larger for higher base SSTs. The relationship between the SST forcing and base SST can be parameterized with the moist static energy model. Future endeavors to quantify feedbacks between the SST and hydrological cycle will be presented with the aim of improving model simulations of tropical air-sea interaction.

Keywords: tropical precipitation variability, SST forcing, air-sea relationship

Intense thunderstorms and their large-scale environments over different regions

*Nana Liu¹

1. Texas A&M University-Corpus Christi

During the past decades, the global precipitation systems has been extensively studied with ground based, ship based, airborne, and space borne radars. Especially with TRMM precipitation radar, Houze and his research group have examined convection over various selected regions, including the South Asian (Romatschke et al.2010; Medina et al. 2010), the South America (Rasmussen and Houze 2011), the Central Africa (Zuluaga and Houze 2015), the Indian and West Pacific oceans (Zuluaga and Houze 2013, Barnes et al. 2015), the Atlantic and East Pacific (Zuluaga and Houze 2015), as well as global (Houze et al. 2015). A general impression from these studies is that convection over various regions not only has their own special dynamic environment setups, but also shares some common features. For example, the most intense convection often occurs over basins downstream of mountains when dry warm air at mid troposphere is above a warm moist air continuously being replenished by a low level jet, which appears locally as a famous storm favoring “onion shape sounding” . The question is whether we can/ how to utilize these common features to improve the numerical models, such as cumulus parameterization. To answer this question, first we examine the relationships between large-scale thermodynamic parameters and sub grid scale convective properties, such as intensity. Then we attempt to understand the importance of specific thermodynamic factors favoring intense convection over various regions. The properties of 16-year of TRMM Precipitation Features are analyzed along with the large-scale parameters from 0.75° ERA-Interim reanalysis. The environment variables, including CAPE, CIN, low level wind shear, lift condensation level, among many others, are individually as well as jointly correlated with fractional occurrence of strong convection with high lightning flash rates. Using these relationships, the global distribution of fractional occurrences of convection with high lightning rates are estimated from ERA-Interim variables and compared to the TRMM derived climatologies. Results suggest that regions favoring the intense convection may be partially explained by the combinations of several important thermodynamic environment factors. This work implies the potential of introducing the convective intensity into the cumulus parameterizations.

Keywords: intense thunderstorm, large-scale environment

Significance of cloud and precipitation in aerosol effect on climate

*鈴木 健太郎¹、竹村 俊彦²、五藤 大輔³

*Kentaroh Suzuki¹, Toshihiko Takemura², Daisuke Goto³

1. 東京大学大気海洋研究所、2. 九州大学応用力学研究所、3. 国立環境研究所

1. Atmosphere and Ocean Research Institute, University of Tokyo, 2. Research Institute for Applied Mechanics, Kyushu University, 3. National Institute for Environmental Studies

Aerosol impacts on Earth's climate are still subject to large uncertainty. A major part of this uncertainty arises from atmospheric processes relevant to cloud and precipitation. This is fundamentally due to a dominant role of moist processes in Earth's atmosphere. This study explores how aerosol's impacts on climate are significantly modulated by the presence of cloud and precipitation. For this purpose, numerical experiments are performed with two global models, i.e. (i) MIROC and (ii) NICAM-Chem. The former is a traditional type of global climate model and the latter is a global non-hydrostatic atmospheric model, both of which are coupled to the SPRINTARS aerosol transport module. In the simulations, emissions of scattering (i.e. sulfate) and absorbing (i.e. black carbon) aerosols are separately perturbed with uniform factors multiplied to investigate the climate responses to perturbations of each aerosol type. The results are analyzed in the context of global energy budget to find that energy budget components respond differently to perturbations of scattering and absorbing aerosols due to different responses of cloud and precipitation. The cloud response to perturbations of absorbing aerosols is found to produce a negative radiative effect that significantly reduces the original positive radiative forcing of the aerosols whereas the cloud response to scattering aerosols tends to enhance the original cooling effect of the aerosols via aerosol-cloud interactions. The two types of aerosols also cause distinctly different responses of precipitation through different pathways of energy budget modulations occurring over different time scales. These results underscore a significance of cloud and precipitation processes in quantification of aerosol impacts on global climate and may help reduce a large inter-model spread in estimates of the hydrologic sensitivity in climate predictions.

キーワード：雲、エアロゾル、エネルギー収支、気候モデル

Keywords: cloud, aerosol, energy budget, climate model

A statistical comparison of precipitation feature characteristics over land and oceans utilizing the GPM DPR data

*小野 茉莉花¹、高薮 縁¹

*Marika Ono¹, Yukari Takayabu¹

1. 東京大学 大気海洋研究所

1. Atmosphere and Ocean Research Institute, the University of Tokyo

The relationship between tropical (30N-30S) and extratropical (30N-65N, 30S-65S) precipitation feature characteristics and the environment, such as an atmospheric moisture field, is analyzed focusing on a comparison over land and oceans using the GPM (Global Precipitation Measurement) DPR (Dual-frequency Precipitation Rader) data.

The difference between over land and the oceans is observed in terms of the relation between daily column relative humidity (CRH) derived from ERA-interim data and precipitation feature characteristics obtained from the GPM DPR. Over tropical oceans, volumetric precipitation and stratiform precipitation area of precipitation features rapidly increase with CRH, as reported in previous studies. Over tropical land, on the other hand, volumetric precipitation of precipitation feature has a peak at around CRH 0.7. In terms of the relationship to CRH, we also analyzed tropical and extratropical precipitation feature characteristics. Over tropical oceans, a class of well-organized precipitation systems observed in the highly humid environment has the largest contribution to total precipitation. In contrast, highly convective precipitation systems observed in moderately humid conditions substantially contribute to total precipitation over land.

Over land, it is considered that the heated land surface during daytime is likely to prepare more unstable lower troposphere and thicker mixed layer compared to the case over ocean. Such unstable conditions can lead to the initiation of convective clouds. Therefore regional analysis about environment has been conducted from the perspective of a comparison in various CRH conditions and seasons. In the Amazon, for example, precipitation features observed in moderately humid conditions are dominant in the premonsoon season. In addition, lower troposphere is in most unstable condition in Amazonian premonsoon season. It is suggested that relatively lower humid conditions seasonally coexist with more unstable conditions. This result implies a possibility that the peak in volumetric precipitation of precipitation features at moderate CRH is associated with convective systems developed in such unstable conditions.

In mid-latitude regions, the different results between over land and over oceans are also observed. Over extratropical oceans, volumetric precipitation and stratiform precipitation area of precipitation features also increase with CRH as over tropical oceans. However, the relationship is relatively linear over extratropical oceans in contrast to an exponential growth observed over tropical oceans. It is possibly attributed to the difference in dominant precipitation mechanism between tropics and mid-latitude regions. Over extratropical land, volumetric precipitation of precipitation features has a peak at around CRH 0.55-0.65. This result over extratropical land is similar to that over tropical land. This agreement of results can be explained by the fact that highly convective systems greatly contribute to total precipitation over both land regions.

キーワード：衛星降水観測、GPM DPR、降水特性

Keywords: Satellite Precipitation Measurements, GPM DPR, Precipitation Characteristics

東太平洋ITCZの順圧不安定場の解放と再構築に関する時間変動の解析 Analysis of the Time Development on Release and Reconstruction of Barotropic Instability Field in the ITCZ in the Eastern Pacific Ocean

*河田 裕貴¹、高薮 縁²、濱田 篤²

*Yuki Kawata¹, Yukari Takayabu², Atsushi Hamada²

1. 東京大学理学部地球惑星物理学科、2. 東京大学大気海洋研究所

1. Department of Earth and Planetary Science, School of Science, The University of Tokyo, 2. Atmosphere and Ocean Research Institute, The University of Tokyo

東太平洋ITCZは、力学的なシア不安定により東西一様な雲の帯が時折breakdownを起こして複数の低気圧性擾乱を生成することが知られている。先行研究では、数値シミュレーションによる現象理解が多く、観測データを使った定量的解析はあまり例がなかった。本研究では観測データを使ってポテンシャル渦度（PV）収支解析を行い、東太平洋ITCZのbreakdownと場の再構築の時間発展の様子の定量化を試みた。

利用したデータは欧州中期気象予報センターの再解析ERA-interim(ERA-I)（6時間毎）、熱帯降雨観測衛星（TRMM）降雨レーダデータから推定された三次元非断熱加熱（SLH ver.7）、GSMaP地表面降水（1時間毎）である。水平空間解像度はERA-Iが緯度・経度幅0.75度、TRMMのデータが約5km、GSMaPデータが緯度・経度幅0.1度である。

TRMM SLHデータのサンプリングが限られるため、GSMaP降水データから、参照テーブルを用いて非断熱加熱を求める方法を考えた。まず降水強度を強さ別に3クラスに分け、500hPaの鉛直風に対して非断熱加熱の鉛直分布を与えるテーブルを作成した。その後、GSMaPとテーブルを使いながらITCZ域の非断熱加熱量を求めた。最後に、非断熱加熱の鉛直プロファイルからその場でのPV生成を定量化し、ERA-Iの力学場と共に、ITCZ域のPV収支解析を行った。

まずはITCZのbreakdownの例として引用されることの多い1988年7月から8月にかけてのイベントを、再解析データERA-Iを用いて解析した。基本場・擾乱場を分離する処理を行った結果、初期状態の東西一様な高渦位帯の状態では順圧不安定の必要条件を満たしており、その後生じる擾乱の発達に伴って不安定が解消されていく様子を捉えることができた。

次に2003年の8月に起こったイベントを解析した。その結果、東太平洋ITCZ域では雄大積雲による高度2km付近の非断熱加熱量が大きく、breakdown初期には加熱が極大を迎えることが確認できた。擾乱がITCZ域から抜けていくのに従って加熱量は落ち着き、次第に場の回復へと向かう時間変化も捉えることができた。

最後に、下層の非断熱加熱によるPV生成を定量的に見積もり、ITCZ域のPV収支を調べた。850hPa面のPV収支解析の結果、下層のPV生成量はITCZ域の外部からの流入や850hPa面のPV変化量に比べて非常に大きいことがわかった。このことから、下層で形成されたPVが鉛直へと輸送された可能性が考えられたため、次に鉛直方向のPV収支を調べた。300hPa面、500hPa面をそれぞれ上層、中層を代表する気圧面とし鉛直3層の近似をした結果、breakdownイベントの初期に下層で生成された過剰なPVは、上層へと輸送されて中層・上層のPV強化を助けていることが示唆された。場の回復へ向かうとPVの鉛直輸送はあまり確認できなくなっていく、下層で生成したPVはその場の回復に使われていることも示唆された。

今後は、本研究の解析に用いたデータの不確定性の検討も行っていきたい。

キーワード：熱帯収束帯、順圧不安定、衛星データ解析、非断熱加熱

Keywords: Intertropical Convergence Zone, Barotropic Instability, Analysis of the satellite data, Diabatic Heating

Characteristics and regional differences of summer warm rain over the tropical and subtropical pacific ocean observed by TRMM

*Fang Qin¹

1. University of Science and Technology of China

Based on the merged measurements from the TRMM Precipitation Radar and Visible and Infrared Scanner, refined characteristics (intensity, frequency, vertical structure and diurnal variation) and regional differences of the warm rain over the tropical and subtropical Pacific Ocean (40°S-40°N, 120°E-70°W) in boreal summer are investigated for the period 1998-2012. The results reveal that three warm rain types (phased, pure and mixed) exist over these regions. The phased warm rain, which occurs during the developing or declining stage of precipitation weather systems, is located over the central to western Intertropical Convergence Zone, South Pacific Convergence Zone, and Northwest Pacific. Its occurrence frequency peaks at midnight and minimizes during daytime with a 5.5-km maximum echo top. The frequency of this warm rain type is about 2.2%, and it contributes to 40% of the regional total rainfall. The pure warm rain is characterized by typical stable precipitation with an echo top lower than 4 km, and mostly occurs in Southeast Pacific. Although its frequency is less than 1.3%, this type of warm rain accounts for 95% of the regional total rainfall. Its occurrence peaks before dawn and it usually disappears in the afternoon. For the mixed warm rain, some may develop into deep convective precipitation, while most are similar to those of the pure type. The mixed warm rain is mainly located over the ocean east of Hawaii. Its frequency is 1.2%, but this type of warm rain could contribute to 80% of the regional total rainfall. The results also uncover that the mixed and pure types occur over the regions where SST ranges from 295 to 299 K, accompanied by relatively strong downdrafts at 500 hPa. Both the mixed and pure warm rains happen in a more unstable atmosphere, compared with the phased warm rain.

Keywords: warm rain, frequency, diurnal variation, radar reflective factor, trade wind

CloudSat/CALIPSO併用データから得られた北太平洋上の多層雲特性について

Multilayer Cloud Characteristics over the North Pacific Ocean Obtained from CloudSat/CALIPSO Combined Data

*山内 晃¹、河本 和明¹、岡本 創²

*Akira Yamauchi¹, Kazuaki Kawamoto¹, Hajime Okamoto²

1. 長崎大学院水産・環境科学総合研究科、2. 九州大学応用力学研究所

1. Graduate School of Fisheries and Environmental Sciences, Nagasaki University, 2. Research Institute for Applied Mechanics, Kyushu University

Clouds have a large impact on the hydrological system and Earth's energy budget. Many previous studies identified clouds as an important source of uncertainty when attempting to understand and predict global climate change (*e.g.*, Stephens, 2005; Dufresne and Bony, 2008). Cloud effects are strongly regulated by their microphysical (particle size, number concentration, and mass density of water or ice particulates) and macrophysical (temporal frequency, height, geometrical thickness, and rainfall intensity) structures. For example, Kawamoto and Hayasaka (2008) reported that surface radiative flux was dominated by cloud optical thickness and cloud cover. However, in the case of a structure where the upper cloud and the lower cloud vertically overlap, the influence of the upper cloud on the lower cloud is not known in detail.

In this study, we investigated the difference in the cloud geometrical thickness and maximum radar reflectivity between single and double layered-clouds. As a result, we found that lower cloud of the double layered-clouds were geometrically thinner than the single layer clouds, and those radar reflectivity decreased. Significant differences were observed when the upper clouds were geometrically thick. Altostratus clouds were dominated in the upper clouds over the northern part of the North Pacific Ocean, and upper clouds were geometrically and optically thicker than in other regions. Therefore, we concluded that growth suppression effect was strongly observed in this region.

キーワード：多層雲、CloudSat/CALIPSO、北太平洋

Keywords: Multilayer Cloud, CloudSat/CALIPSO, North Pacific Ocean

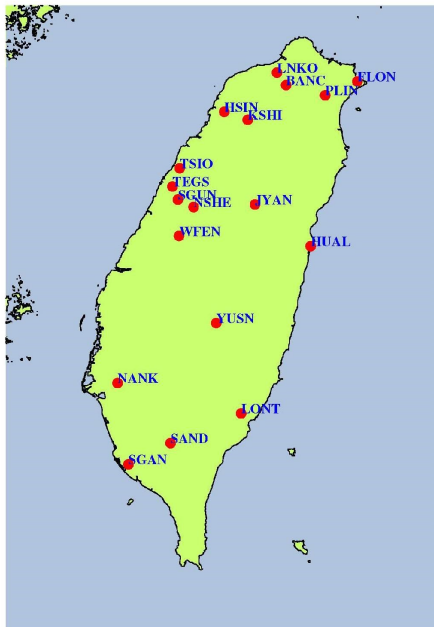
Feasibility Assessment of Heavy Rainfall Forecast Using GPS-Derived ZTDs

*LiChun Tseng¹, Shen Yu Hsiao¹, ChunMin Shih¹, LiPing Li¹, Chang Jung Chieh¹, FENG SHIH LIN¹

1. National Chung Hsing University

This study focuses on the correlation between Zenith Total Delays (ZTDs) derived from global positioning system (GPS), and rainfalls. The feasibility assessment of heavy rain forecast by GPS-derived ZTDs during typhoon events are subsequently analyzed. The study period are selected during the strong typhoon events in recent years. We use the method of Point Precise Positioning (PPP) with the software “Bernese 5.2” to compute ZTDs in 129 GPS stations during study period. The ZTD results are both compared with those from University of the Atmospheric Research (UCAR), and the rainfall data from the rainfall stations of Central Weather Bureau, Taiwan. We currently have preliminarily analyzed the correlation between ZTDs and the rainfalls at 18 GPS-rainfall stations (See the attached Figure) during the period of Typhoon Soudelor, 2015. We conclude that heavy rain forecast by GPS-derived ZTD has great potential and it is worth doing further research for typhoon disaster prevention.

Keywords: GPS, ZTD, heavy rain forecast, typhoon disaster prevention



Remote Sensing of the Davao atmosphere using GNSS and radiosonde data for 2013-2015

Kristine Mae Rodriguez Carnicer¹, *Maria Cecilia Dandan Galvez¹, Rui M.S. Fernandes², Edgar Amemita Vallar¹

1. Environment and Remote sensing Research (EARTH) Laboratory, Physics Department, De La Salle University, Manila, 2. Space and Earth Geodetic Analysis Laboratory (SEGAL), University of Beira Interior, Portugal

One GNSS receiver installed at Davao University was utilized to obtain estimates of the atmospheric water vapor content in Davao City for the years 2013-2015. The datasets from the local radiosonde station was used to verify the measured GNSS-derived precipitable water vapor (PWV) and a significantly strong correlation ($R=0.871$) was calculated. The parameter water vapor weighted mean temperature, T_m is a significant factor in deriving PWV values from GNSS satellite data. A local T_m model utilizing the datasets from the Davao City radiosonde station was derived and validated by comparison to the global and regional models. Time series plots were made out of the calculated GNSS PWV values for the years 2013, 2014 and 2015 to test for any annual, seasonal and monthly variations. Results from analysis of variance (ANOVA) with post-hoc tests showed that significant differences were measured in the PWV means for the three years tested. There were also significant differences in the PWV averages for the dry and wet season as well as between the cool dry, hot dry and wet seasons. The results for the monthly variations agree well with the wet and dry seasons with the month of February (2013-2015) getting the lowest average monthly value of GNSS PWV and the months of May (2013, 2015) and June (2014) the highest. The temporal behavior of GNSS PWV was also evaluated for moderate to torrential rain events. It was shown that while moderate rain follows small variations in PWV, heavy torrential rains usually follow a peak in the PWV value with a time lag ranging from 2 –8 hours.

Keywords: GNSS, Atmospheric Water vapor, rain events

The analysis of Taiwan dry-season precipitation patterns and frontal system variations

*Shih-Hao Su¹, Bing-Kui Chiou¹, Jung-Lien Chu², Lee-Yaw Lin²

1. Chinese Culture University, 2. National Science and Technology Center for Disaster Reduction

Generally, there is relative less precipitation during the months between winter to next spring, December to April, in Taiwan. Therefore, we usually define these months as dry-season. The historical drought events show that most events are occurred between February to April and lead to a huge economic loss in agriculture. The major synoptic weather events which affect Taiwan during this period is the frontal system. Therefore, understanding the correlation between the spatial-temporal variations of frontal systems and the seasonal rainfall amount and frequency is important.

In this study, the surface weather maps were used as the subjective analysis of synoptic scale frontal systems, which affected Taiwan, from 1980 to 2015. We also used the hourly data of precipitation from 21 meteorological stations in Taiwan which operated by the Central Weather Bureau (CWB). Those stations are equally distributed over the island which including 5 mountain stations. The rainfall distribution of 21 stations is approximate match with detailed rain gauge observations and only may underestimated over the CMR southern slope.

The preliminary results show that the frontal systems have strong inter-annual variations in spatial and temporal characteristics for both front numbers and affecting days and there was a decreasing trend in past 36 years. We also noticed that the frontal properties have different varies between the seasons which may related to the temporal and spatial shifting of the large-scale circulations. Generally, 25% of days per year were affected by the frontal system. Moreover, 40% to 50% days during the Spring and Mei-Yu season were also affected by frontal system. The average affecting duration of each front was 12-24hrs of the Mei-Yu season and about 5hrs for other seasons.

The spatial and temporal variations of frontal systems were correlated to the seasonal precipitation. The seasonal total rainfall amount in the dry-season has significant correlation with the frontal numbers and frontal days (0.56/0.55). As speculation, the frontal extreme rainfall events are also highly related to the frontal numbers and days during the dry-season. Furthermore, we observed that there are two different types of precipitation patterns associated with frontal system. The extreme rainfall events are highly associated with frontal-terrain which is induced deep convections and the light/moderate rainfall are related with the stratiform components.

We also noticed that there are some large-scale patterns which may also play important roles to influence the spatial and temporal variations of frontal systems in Taiwan. The preliminary results show that large-scale patterns are different between seasons. For example, there is a low-level of anticyclonic circulation anomaly at northwest pacific region during the winter time for more fronts year, but it will change to the cyclonic circulation anomaly for more fronts year in spring time. The south-west flow also show an obvious feature for more fronts year in spring time.

Keywords: Dry-season precipitation, Subjective front analysis, Precipitation patterns, Extreme rainfall events

Statistical analysis of regional rainfall distributions around isolated Island by low-level winds during the winter season

*Gyeong-Tae Ryu¹, Dong-In Lee¹, Keun-Ok Lee³, Dong-Kyun Kim², Cheol-Hwan You⁴

1. Division of Earth Environmental System Science Pukyong National University, Busan, Korea, 2. Department of Environmental Atmospheric Sciences, Pukyong National University, Korea, 3. LATMOS/IPSL, UPMC Univ. Paris 06, Sorbonne Universités, UVSQ, CNRS, Paris, France, 4. National Research Center for Disaster-free and Safe Ocean City, Dong-A University, Busan, Korea

In Korea, rainfall systems passing over an isolated mountain tend to develop by orographic effects. We statistically analyzed regional rainfall distributions according to wind characteristics at low levels (925–850 hPa) during winter seasons in 2009–2016 around Jeju Island which is elliptically shaped and oriented from the west-southeast to east-northeast direction with a height of 2 km, width of 35 km, and length of 78 km. For this study, rain gauge data at 26 sites, two operational S-band Doppler radar data, and mesoscale analysis model data were used.

The accumulated rainfall was recorded by the 26 rain gauges during December–February from 2009 to 2016. The accumulated rainfall maximum larger than 40000 mm appeared on the mountain crest (altitude > 1.25 km). In contrast, the region of the accumulated rainfall less than 15000 mm appeared on the western coast of Jeju Island. This means that the rainfall distributions were affected by the mountainous region in Jeju Island. For radar data analyses, 3-Dimensional CAPPI radar data during precipitation periods were used. To determine a representative environmental wind on Jeju Island, the MSM-GPV (Mesoscale Model-Grid Point Value) data between 850 hPa and 925 hPa levels were used. By wind direction and wind speed, CAPPI radar data were classified into 32 wind categories. The 2 km-CAPPI radar reflectivities were time-averaged in each category.

In this study, characteristics of regional rainfall distributions classified into the 32 wind categories by wind direction and speed were investigated. The most of high rainfall frequencies occurred when the northwesterlies (51.6%) and northerly winds (16.0%) prevailed at low-levels. Rainfall frequencies at westerlies (8.6%) and southwesterlies (7.5%) were relatively low. At relatively strong northwesterlies ($SPD > 10 \text{ m s}^{-1}$), rainfall systems that moved from the offshore region have developed on mountain slope. When the relatively weak southwesterlies ($5 \text{ m s}^{-1} < 10 \text{ m s}^{-1}$) and strong southwesterlies ($SPD 20 \text{ m s}^{-1}$) were dominant, there were high rainfall distributions on the top of the mountain and the southern upslope, respectively. Similarly, when the relatively weak southerly winds ($5 \text{ m s}^{-1} < SPD 10 \text{ m s}^{-1}$) and strong southerly winds ($SPD 20 \text{ m s}^{-1}$) prevailed, high rainfall frequencies were concentrated on the top of the mountain and the southern upslope, respectively. Therefore, the development of rainfall systems that pass over the mountain around the Jeju Island seems to be closely related to the characteristics of wind direction and wind speed at low-levels.

Acknowledgements

This work was funded by the Korea Meteorological Industry Promotion Agency under Grant KMIPA 2015-5060 and the BK21 plus Project of the Graduate School of Earth Environmental Hazard System.

Keywords: regional rainfall distribution, isolated elliptical terrain, low-level wind

Statistical analysis of regional rainfall distributions around isolated Island by low-level winds during the winter season

Gyeong-Tae Ryu¹, Dong-In Lee^{1*}, Keun-Ok Lee³, Dong-Kyun Kim², Cheol-Hwan You⁴

¹*Division of Earth Environmental System Science Pukyong National University, Busan, Korea*

²*Department of Environmental Atmospheric Sciences, Pukyong National University, Korea*

³*LATMOS/IPSL, UPMC Univ. Paris 06, Sorbonne Universités, UVSQ, CNRS, Paris, France*

⁴*National Research Center for Disaster-free and Safe Ocean City, Dong-A University, Busan, Korea*

Abstract

In Korea, rainfall systems passing over an isolated mountain tend to develop by orographic effects. We statistically analyzed regional rainfall distributions according to wind characteristics at low levels (925–850 hPa) during winter seasons in 2009–2016 around Jeju Island which is elliptically shaped and oriented from the west-southeast to east-northeast direction with a height of 2 km, width of 35 km, and length of 78 km. For this study, rain gauge data at 26 sites, two operational S-band Doppler radar data, and mesoscale analysis model data were used.

The accumulated rainfall was recorded by the 26 rain gauges during December–February from 2009 to 2016. The accumulated rainfall maximum larger than 40000 mm appeared on the mountain crest (altitude > 1.25 km). In contrast, the region of the accumulated rainfall less than 15000 mm appeared on the western coast of Jeju Island. This means that the rainfall distributions were affected by the mountainous region in Jeju Island. For radar data analyses, 3-Dimensional CAPPI radar data during precipitation periods were used. To determine a representative environmental wind on Jeju Island, the MSM-GPV (Mesoscale Model-Grid Point Value) data between 850 hPa and 925 hPa levels were used. By wind direction and wind speed, CAPPI radar data were classified into 32 wind categories. The 2 km-CAPPI radar reflectivities were time-averaged in each category.

In this study, characteristics of regional rainfall distributions classified into the 32 wind categories by wind direction and speed were investigated. The most of high rainfall frequencies occurred when the northwesterlies (51.6%) and northerly winds (16.0%) prevailed at low-levels. Rainfall frequencies at westerlies (8.6%) and southwesterlies (7.5%) were relatively low. At relatively strong northwesterlies ($SPD > 10 \text{ m s}^{-1}$), rainfall systems that moved from the offshore region have developed on mountain slope. When the relatively weak southwesterlies ($5 \text{ m s}^{-1} < SPD \leq 10 \text{ m s}^{-1}$) and strong southwesterlies ($SPD \geq 20 \text{ m s}^{-1}$) were dominant, there were high rainfall distributions on the top of the mountain and the southern upslope, respectively. Similarly, when the relatively weak southerly winds ($5 \text{ m s}^{-1} < SPD \leq 10 \text{ m s}^{-1}$) and strong southerly winds ($SPD \geq 20 \text{ m s}^{-1}$) prevailed, high rainfall frequencies were concentrated on the top of the mountain and the southern upslope, respectively. Therefore, the development of rainfall systems that pass over the mountain around the Jeju Island seems to be closely related to the characteristics of wind direction and wind speed at low-levels.

Acknowledgements

This work was funded by the Korea Meteorological Industry Promotion Agency under Grant KMIPA 2015-5060 and the BK21 plus Project of the Graduate School of Earth Environmental Hazard System.

Keywords: regional rainfall distribution, isolated elliptical terrain, low-level wind

Topographic effects on spatiotemporal variations of short-duration rainfall events in warm season of central North China

*Weihua Yuan¹, Yu Rucong², Sun Wei¹, Chen Haoming²

1. LASG, Institute of Atmospheric Physics, Chinese Academy of Sciences, 2. Chinese Academy of Meteorological Sciences

Statistical analyses of the hourly station rainfall observation over the recent 8 years show that rainfalls in the warm season (May-October) of the central North China are dominated by short-duration rainfall events (lasting less than or equal to 6 h) and the southeastward delayed diurnal phases of total rainfall revealed by previous studies are mainly contributed by the propagating short-duration rainfall rather than the long-duration rainfall as that along the Yangtze River Valley. The spatiotemporal features of rainfall events are highly correlated with elevation heights. The largest frequency of short-duration rainfall events locates in the southeastern inner periphery of Taihangshan and Yanshan mountains. Rainfall over the northwestern mountains often occurs in the afternoon. Some rainfall events propagate southeastward and influence the rainfall in the southeastern foothills and plain. The rainfall with short duration time mainly begins around the late evening in the southeastern plain, and even later in coastal regions. The understanding of topographic effects to rainfall events is discussed based on reanalysis and station data. Results indicate that the topography influences the diurnal varied surface or low-level temperature, moisture and wind fields, which benefit rainfall events occurring in the afternoon over the northwestern mountains firstly and the southeastward propagation afterward.

Keywords: Short-duration precipitation, Topographic effects, hourly precipitation data

Does the climate warming hiatus exist over the Tibetan Plateau?

*Anmin Duan¹

1. Institute of Atmospheric Physics, Chinese Academy of Sciences

The surface air temperature change over the Tibetan Plateau has been determined based on historical observations from 1980 to 2013. In contrast to the cooling trend in the rest of China, and the global warming hiatus post-1990s, an accelerated warming trend has appeared over the Tibetan Plateau during 1998–2013 ($0.25\text{ }^{\circ}\text{C decade}^{-1}$) compared with that during 1980–1997 ($0.21\text{ }^{\circ}\text{C decade}^{-1}$). Further results indicate that such an accelerated warming trend might be attributed to the cloud-radiation feedback, to some degree. The increased nocturnal cloud over the northern Tibetan Plateau will warm the nighttime temperature by the enhancement of atmosphere counterradiation, while the decreased daytime cloud over the southern Tibetan Plateau will induce the daytime sunshine duration increased, resulting surface air temperature warming. Meanwhile, the in situ surface wind speed has recovered gradually since 1998, and the energy concentration cannot explain the accelerated warming trend. It is suggested that the cloud–radiation feedback may play an important role in modulating the accelerated warming trend over the Tibetan Plateau.

Keywords: Tibetan Plateau, warming amplification , cloud-radiation feedback

Sensitivity of the surface parameters in CReSS for weather simulations over the arid and semi-arid regions

*WoonSeon JUNG¹, Masataka MURAKAMI¹, Taro SHINODA¹

1. Institute for Space-Earth Environmental Research, Nagoya University

To conduct forecast and/or hindcast simulations for rain enhancement research over the United Arab Emirates (UAE), we need an accurate and reliable numerical model to simulate clouds formation and precipitation development over the desert areas. The main purpose of this study is to check the performance of Cloud Resolving Storm Simulator (CReSS: Tsuboki and Sakakibara, 2007) model and validate and improve the numerical model for weather simulations over the UAE.

Land surface temperature plays an important role in reproducing clouds and precipitation, especially over the desert areas. In spite of importance of land surface temperature, CReSS had not been validated in terms of land surface temperature in detail and it recently turned out that CReSS experiments underestimate the land surface temperature during not only daytime but also nighttime.

To investigate the major parameters to influence the land surface temperature, sensitivity test was performed for the time duration from 0600 UTC 09th to 0600 UTC 12th September 2015 and compared with Aqua/Moderate Resolution Imaging Spectroradiometer (MODIS) data. The parameters related to land surface processes, which were investigated in this study, were thermal diffusivity, thermal capacity, evapotranspiration efficiency, roughness length, soil temperature in the deepest layer, emissivity on surface, number of soil and sea layers, and thickness of each soil layer.

The sensitivity experiments showed that the increase of land surface temperature in the daytime resulted from smaller thermal diffusivity, thermal capacity, evapotranspiration efficiency, roughness length, emissivity of land surface and larger soil temperature in the deepest layer, number of soil layers and thickness of soil layers. On the other hand, the increase of land surface temperature in the nighttime resulted from smaller evapotranspiration efficiency, emissivity of land surface and larger thermal diffusivity, thermal capacity, soil temperature in the deepest layer, number of soil layers, thickness of soil layers.

On the basis of sensitivity experiment, numerical experiments were performed to optimize the parameters in trial and error manner. To increase the land surface temperature during both daytime and nighttime, diverse parameters were tuned, including soil temperature at the deepest layer, evapotranspiration efficiency, and so on. The difference of domain-averaged land surface temperatures between Aqua/MODIS observation and CReSS simulation decreased from 13 K in the experiments with default values of the parameters (CTL) to 1 K in the experiment with optimized values of the parameters (OPT) in the daytime (1400 LST 10 September 2015). The difference in the nighttime (0200 LST 11 September 2015) also decrease from 3 K in CTL to 1 K in OPT experiments (see Figure. 1).

CReSS CTL experiments with 5 km horizontal resolution showed an improvement in reproducing the convective clouds over the desert areas to some extent, but still significantly underestimated such convective clouds. To examine a grid size dependency of the reproducibility of clouds and precipitation over the desert areas, CReSS OPT experiment with 1km horizontal resolution was performed. The model well reproduced convective precipitation over the mountain area and also over northwestern coastal and inland desert areas, which was not well reproduced by CReSS OPT with 5km horizontal resolution.

Keywords: Cloud Resolving Storm Simulator (CReSS), Land surface temperature, United Arab Emirates (UAE)

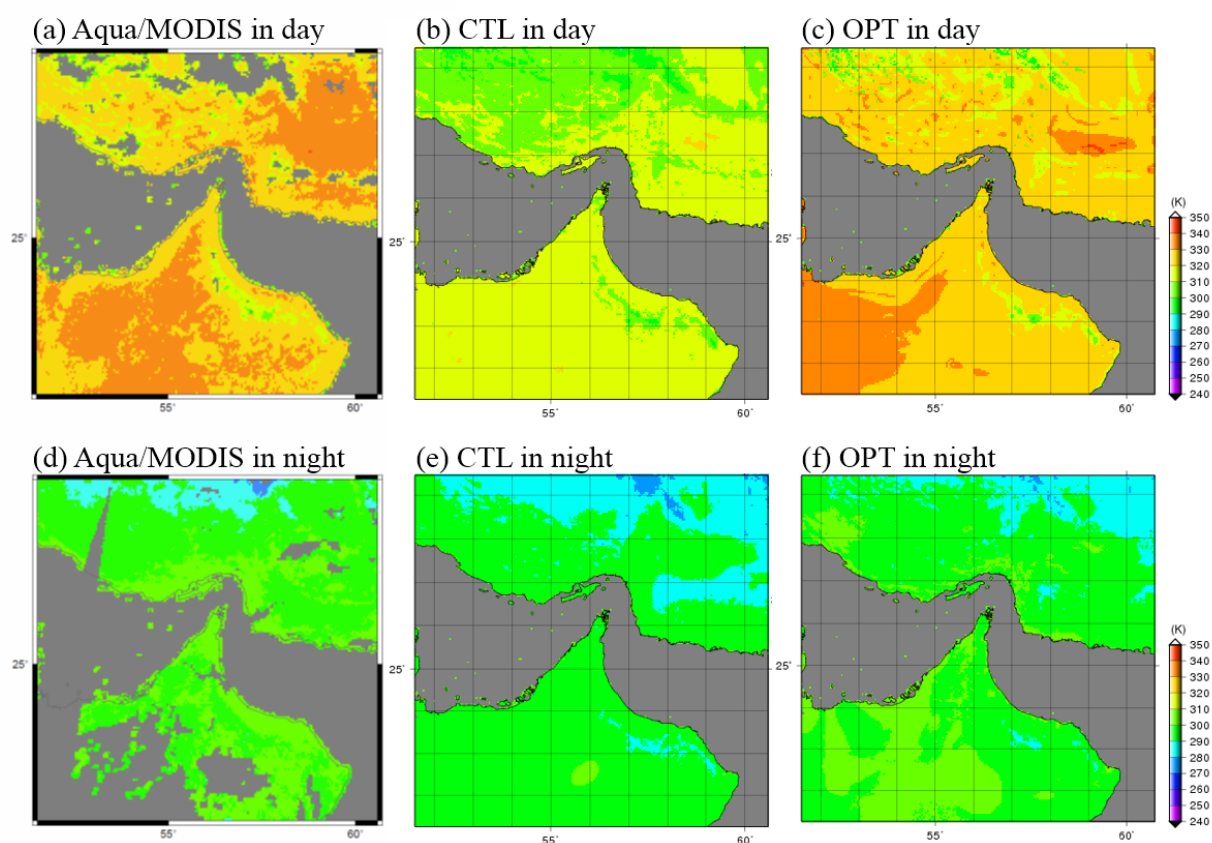


Figure 1. The distribution of land surface temperature by (a) Aqua/MODIS, (b) CReSS CTL, (c) CReSS OPT in 1400 LST 10 September 2015 and (d) Aqua/MODIS, (e) CReSS CTL, (f) CReSS OPT in 0200 LST 11 September 2015.

The role of soil moisture in convective rains in the central region of Mexico

*Edgar Dolores¹, Ernesto Caetano¹

1. National Autonomous University of Mexico

Precipitation in the central region of Mexico during the summer occurs more frequently during the afternoons. Local surface heat and moisture fluxes represent a major source of convective rainfall in Mexico during the summer, driven by positive evaporation-precipitation feedback. The effects of soil moisture are directly reflected in the limitation of evapotranspiration, affecting the development of the planetary boundary layer and, therefore, the initiation and intensity of convective precipitation. This study presents preliminary analysis of the role of soil moisture in convective rains in central Mexico, for which a methodology for the detection of convective initiations similar to Taylor (2015) has been considered. The results show that the moisture fluxes from the surface influence the development of convection favored by mesoscale circulations at low levels. Initiations are more frequent in regions less humid than their surroundings with the very strong signal during the month of September.

Keywords: soil moisture, convective precipitation, mesoscale

Investigation of soil moisture - afternoon precipitation coupling in summer over the Tibetan Plateau using satellite observations

*xianhong Meng¹, Shihua Lyu², Tangtang Zhang¹, Lan Luan¹

1. NIEER CAS, 2. It Univ.

Coupling between soil moisture and afternoon precipitation in summer over the Tibetan Plateau (TP) was investigated using a previously implemented convective triggering potential (CTP)–humidity index (HI) framework by combining satellite observations, including the Atmospheric Infrared Sounder (AIRS), the merged active and passive soil moisture products from the European Space Agency (ESA), and the U.S. Climate Prediction Center (CPC) merged satellite rainfall product (CMORPH). We found that a main atmosphere controlled region was mainly located in the south and the north edge of the TP, and a main negative feedback of soil moisture –afternoon precipitation was in the west of the TP, where the CTP over this region is relatively larger in most time. In the central and the northeast of the TP, both positive and negative feedbacks coexist, with the main positive feedback was shown in the central TP. In addition, the coupling between soil moisture and afternoon precipitation was affected by the statement of monsoon. With the water vapor transport of the monsoon, it is benefit for the co-existence of both positive and negative feedback converting to the positive feedback predominant.

Keywords: Tibetan Plateau, Soil moisture , afternoon precipitation, Satellite observations

Numerical studies of aerosol impact on warm rain using a cloud resolving model with the super droplet method

森木 和也¹、島 伸一郎²、*坪木 和久¹

Kazuya Moriki¹, Sin-ichiro Shima², *Kazuhisa Tsuboki¹

1. 名古屋大学宇宙地球環境研究所、2. 兵庫県立大学

1. Institute for Space-Earth Environmental Research, Nagoya University, 2. Graduate school of Simulation Studies, University of Hyogo

It is well known aerosols affect formation and behavior of clouds. Albrecht (1989) showed that precipitation amount decreases and the cloud lifetime increases with high number concentration of aerosol while precipitation amount increases and cloud lifetime decreases with smaller number concentration of aerosol. To properly consider the interaction of aerosol and clouds, a detailed numerical simulation based on basic physical laws is necessary. In particular, impacts of aerosol on a very intense rainfall of about 100 mm from a warm rain should be studied using a detailed cloud model with resolving size distribution of particles (e.g. aerosol, cloud, and precipitation droplets). Takahashi et al. (1989) investigated precipitation process over the ocean near the Island of Hawaii using a numerical model with a bin method. They found that the process of drizzle is important for heavy rain formation. In the present study, we studied this type of heavy rain and an aerosol impact on the heavy rain.

We coupled the Super Droplet Method (SDM, Shima 2008; Shima et al., 2009) with the Cloud Resolving Storm Simulator (CReSS; Tsuboki and Sakakibara 2001; 2002) to calculate the detailed behavior of aerosol, cloud, and precipitation particles. The purpose of this study is to investigate the influence of change in aerosol number concentration on the heavy precipitation system. In the warm rain, water vapor deposition process and the collision and coalescence processes are important for the particle growths. These processes are considered precisely in the SDM. The sounding data of atmosphere used for the initial field was provided by Wyoming University.

Results of numerical experiments conducted with different aerosol number concentrations, time evolution of cloud and rain mixing ratio had changed drastically. In addition, particle size distributions and their temporal changes were obtained in the experiments. It showed that precipitation decreased while cloud increased with the increase of initial aerosol number concentration. When the initial number concentration decreased, precipitation amount increased. Particle growth was observed around a radius of 0.3 mm at the beginning of precipitation formation in the low aerosol concentration case. This indicates formation of drizzle particles and their growth. Particle growth was observed around 0.6 mm while the formation of drizzle was suppressed when the precipitation is in mature stage.

The effect of aerosol on cloud lifetime was suggested for warm clouds. When the initial aerosol number concentration is low [10.5], precipitation was remarkably increased (over 50 mm). On the other hand, no precipitation occurred when the aerosol concentration was 100 times as large as the low concentration case. In this case, evaporation of cloud droplets becomes dominant and the lifetime of cloud decreases.

キーワード：エアロゾル、超水滴法、雲解像モデル

Keywords: aerosol-cloud interaction, super droplet method, cloud-resolving model

REVIEW OF CHARACTERISTICS OF ELECTRIC FIELD PRIOR TO LIGHTNING

*SRICHITRA S¹, SEBIN SABU¹, NORA ELIZABETH JOBY^{3,2}, PREMLET B³

1. TKM COLLEGE OF ENGINEERING KOLLAM, 2. NATIONAL INSTITUTE OF TECHNOLOGY CALICUT, 3. MES KOLLAM

Abstract: A study on the atmospheric electric fields prior to lightning strike was conducted by means of literature survey and data analysis. Study of electric fields is an important tool of lightning research. Electric field mills are used to observe static atmospheric electric fields during fair weather and during storm conditions. Comparisons show significant changes in electric field due to an approaching storm or a thunderstorm. Attempts to comprehend the variations prior to and after a strike has been done by observatories all over and this paper focuses on identifying characteristic changes in atmospheric electric field prior to a lightning strike. The focus is on static electric field variations prior to strike and this points out to the significance of study of electric field varying from a fair weather scenario to generation of bipolar preliminary breakdown pulses which is defined as the dynamic electrical activity inside cloud before strike. It has been explained by means of BIL (Breakdown Intermediate Leader) model as proposed by Clarence and Malan. Simulation experiments done by Carlson and Liang are seen to reproduce the same characteristics as obtained from field data. This paper helps in identifying the characteristic change in atmospheric electric field prior to lightning strike can create a great advantage in lightning prediction.

Keywords: Lightning, Electric field , Prior to strike

AN ANALYSIS OF LIGHTNING RELATED PARAMETERS USING NASA GHRC DATASETS

*Nora Elizabeth Joby¹, Sebin Sabu², Sri Chithra S.², Abraham Mulamootil², Premlet B.³

1. National Institute of Technology Calicut, 2. TKM College of Engineering Kollam, 3. MES Kollam

The relationship between lightning occurrences and other weather parameters, especially the static and dynamic electric fields is explored based on weather datasets provided by NASA. The Global Hydrology Research Centre (GHRC) and the Kennedy Space Centre (KSC), NASA provides datasets of observed atmospheric parameters associated with natural disasters like lightning, hurricanes etc.

The lightning occurrence data is collected from LDAR (Lightning Detection and Ranging) datasets from GHRC and KSC and CGSLSS (Cloud-to-Ground Lightning Surveillance System) from KSC. Static electric field measurements are obtained with Electric Field Mills (EFM) from the AGBFM (Advanced Ground Based Field Mills) datasets. Dynamic Electric field measurements are also made using dipole and capacitive antennas, and data made available in the form of K-changes. This data, which is available along with timestamps and co-ordinates, are analysed for interrelationships and coincident occurrences. Changes in other weather parameters associated with lightning are also observed. Finally, the feasibility of using these parameters for lightning prediction and detection is examined.

Keywords: lightning, electric field, datasets, electric field mills, lightning detection and ranging

A study on effect of weather conditions on cellular signal strength

*Sebin Sabu¹

1. TKM College of Engineering, Kollam, India

Cellphone density is growing at a very fast pace all over the globe. The high phone density among developing nations also poses it as a societal tool. India has a cellphone density of nearly billion and its fast growing too. In this study we are analyzing the effects of weather parameters on cellular signal strength. Rainfall and Temperature are considered in this study. Changing rainfall patterns are causing a heavy toll on India. We study the effects of rainfall and atmospheric temperature over a region on the cellular signal strength quality at the user end. RSSI (Received Signal Strength Indicator) is a measurement of the power present in a received radio signal. Rainfall can cause natural interference over transmitting signals (radio waves) in microwave links. We use SignalStrength Android Application Programming Interface Keys popularly known as APIs to get real-time RSSI readings from smartphones. Rainfall intensity measurements are made by rain gauges and temperature measurements are made by weather station. It has been concluded from the analysis that there is an effect of weather parameters on cellular signal strength measured at the user end. This study raises the potential of using Signal Strength measurements as high-resolution weather analysis over a region. Growing concerns of climatic change can be addressed by improved weather analysis and prediction, this study can be the first step towards weather analysis using cellular signal strength measurement.

Keywords: Rainfall, ClimaticChange, Cellularsignalstrength

Bacterial communities in rainwater associated with different synoptic weather systems at a site in Kumamoto, southwestern Japan

*Wei Hu¹, Kotaro Murata¹, Daizhou Zhang¹

1. Prefectural University of Kumamoto

Bacteria substantially exist in rainwater and can be disseminated by rain from the atmosphere to the earth's surfaces, on the one hand driving the development and evolution of ecosystems, but on the other hand causing great concern for their potential negative impacts on environments and public health. However, studies of bacterial communities in rainwater, especially those dependent on different synoptic weather systems, are largely lacking. In this study, rainwater samples were collected at a site (32.806°N, 130.766°E) in Kumamoto, southwestern Japan. Samples from four cases of each rain types of cyclone-, Meiyu (plum rain) front- and non-Meiyu stationary front-associated rains, and samples from three cases of typhoon-influenced rains were analyzed. The abundance of bacteria in these rainwater samples was $0.8\text{--}4.6 \times 10^4$ cells ml⁻¹, and the viability (the ratio of the abundance of bacteria with intact cell membranes to that of total bacteria) was 66–91%. Bacteria in the rainwater of cyclones, in accompany with the intrusion of continental air, were characterized by high abundance and low viability. In other cases of rain, when clouds were significantly affected by marine air, the concentration of bacteria was low and the viability was high. Bacterial communities in rainwater, identified by using 16S rRNA gene sequencing, were dominated by *Proteobacteria*, *Cyanobacteria*, *Bacteroidetes*, *Firmicutes* and *Actinobacteria* phyla. Diverse bacterial communities were appeared in four types of rainwater samples, and about half of the phyla (17 out of 35) were common in different types of rainwater. The presence of ice nucleation-active bacteria, such as the members of the genera *Pseudomonas*, *Xanthomonas* and *Erwinia*, indicate bacteria as nuclei in clouds were a potential source of bacteria in rainwater. Marine bacterial taxa, e.g., *Pseudoalteromonas*, *Synechococcus* and *Marinobacter*, were detected in rainwater samples, showing that marine bacteria were dispersed via cloud or rainwater.

Keywords: Bacteria, Community composition, 16S rRNA sequencing, Rainwater, Synoptic weather